Changes in the current density–voltage and external quantum efficiency characteristics of n-type single-crystalline silicon photovoltaic modules with a rear-side emitter undergoing potential-induced degradation

Seira Yamaguchi[a,*], Atsushi Masuda[b], Keisuke Ohdaira[a]

[a]*Japan Advanced Institute of Science and Technology (JAIST), Nomi, Ishikawa 923-1292, Japan*
[b]*Research Center for Photovoltaics, National Institute of Advanced Industrial Science and Technology (AIST), Tsukuba, Ibaraki 305-8568, Japan*

Abstract

This study addresses the potential-induced degradation (PID) of n-type single-crystalline silicon (sc-Si) photovoltaic (PV) modules with a rear-side emitter. The n-type rear-emitter module configurations were fabricated using n-type bifacial sc-Si solar cells by module lamination with the p^+ emitter side down. After the PID tests applying −1000 V, the modules show a rapid decrease in the open-circuit voltage (V_{oc}), followed by relatively slower reductions in the fill factor and the short-circuit current density (J_{sc}). Their dark current density–voltage (J–V) data and external quantum efficiencies (EQEs) indicate that the drop in V_{oc} is caused by an increase in the saturation current density due to the enhanced surface recombination of minority carriers. In contrast, the modules exhibit slight degradation under +1000 V, which is characterized by only slight decreases in V_{oc} and J_{sc}. The EQE measurement reveals that these decreases are also attributed to the enhanced surface recombination of minority carriers. This behavior is almost identical to that of the polarization effect in n-type interdigitated back contact PV modules reported in a previous study. By comparing the PID resistance with that of other types of modules, the n-type rear-emitter PV modules are relatively resistant to PID. This may become an advantage of the n-type rear-emitter PV modules.

*Corresponding author
Email addresses: s-yamaguchi@jaist.ac.jp (Seira Yamaguchi), atsushi-masuda@aist.go.jp (Atsushi Masuda), ohdaira@jaist.ac.jp (Keisuke Ohdaira)

Keywords: Potential-induced degradation, n-type single-crystalline silicon photovoltaic module, n-type rear-emitter photovoltaic module, Surface recombination, Polarization effect

1. Introduction

The n-type crystalline silicon (c-Si)-wafer-based solar cells attracted attention owing to their high efficiency potential [1]. As for the p^+ emitter formation in the n-type c-Si solar cells, some different techniques were successfully developed, such as boron-diffused front emitters [2, 3], p-type/i-type amorphous silicon heterojunctions [4–6], and aluminum (Al)-alloyed rear emitters [7–9]. In particular, the Al-alloyed rear emitters can reduce the production costs since the emitters can be formed by the conventional fabrication process for back-surface fields, which was already widely used in the production of the commercial p-type c-Si solar cells. Therefore, Al-alloyed rear-side emitter solar cells are suitable for use in photovoltaic (PV) power plants, such as very large-scale PV (VLS-PV) systems.

To ensure high reliability and long-term stability of PV systems, it is important to understand the possible degradation behavior of the PV modules. In particular, degradation associated with system bias voltage is identified as a central problem in VLS-PV systems with remarkably high system voltage. This degradation is induced by high electrical potential differences between grounded frames and cells, and it is generally referred to as potential-induced degradation (PID). Thereby, modules deployed in the systems can show significant performance losses [10–12].

The PID of p-type c-Si PV modules was well documented by many researchers. In p-type c-Si modules, significant degradation occurs only under negative potential differences from the grounded frames [10–12]. Such negative potential differences result in sodium cations (Na^+) transfer from the cover glass toward the cells, and the Na^+ accumulates on the devices [12]. (There are controversial points on true Na sources. For instance, an experimental result suggests that Na originates from contaminants on the cell surface [13].) In this situation, the Na^+ ions can easily pass even through SiN_x passivation layers, which are known as good diffusion barriers for sodium [14], with the assistance of a strong electric field [15]. The cells contaminated with Na exhibit a reduction in parallel resistance (R_p) [10] and enhancement of depletion-region recombination [16, 17]. This kind of PID is generally referred to as the "PID of shunting type" ("PID-s") [18]. With regard to these facts, Naumann *et al.* [19] discovered that Na accumulates into the silicon nitride (SiN_x)/Si interface of c-Si solar cells in PID-affected regions. It

was also reported that both PID shunts and Na accumulation locally occur at the same spots [20, 21]. Moreover, stacking faults existing near the front surface of c-Si were seen to be decorated by Na, and the Na-decorated stacking faults were found to play a crucial role in PID [22]. Naumann *et al.* and coworkers proposed a physical model that can explain the shunting based on Na-decorated intrinsic stacking faults [18, 22, 23]. Recently, Ziebarth *et al.* [24] discussed in detail the diffusion of Na in the intrinsic staking faults and the short-circuiting of p–n junctions by theoretical calculations based on density functional theory and reported their theoretical findings to be consistent with the experimental results presented by Naumann *et al.* [18, 22].

Regarding the PID of the n-type PV modules, there are several studies on interdigitated back contact (IBC) [25–27] and front-emitter [28] PV modules. It was reported that n-type IBC PV modules degrade under positive bias and that PID-affected modules show decreased open-circuit voltage (V_{oc}) and short-circuit current density (J_{sc}) due to the enhanced surface recombination of minority carriers [25]. Naumann *et al.* showed that n-type IBC PV modules can also degrade under negative bias [26]. In n-type IBC PV modules with a front-floating emitter, a similar degradation was observed under negative bias [27]. Hara *et al.* [28] revealed that the degradation of front-emitter PV modules occurs under negative bias. They found that the n-type front-emitter modules exhibit decreases in V_{oc} and J_{sc}, while maintaining fill factor (FF), and the degradation tends to occur easily under low temperature or a low bias voltage compared with conventional p-type c-Si modules. By contrast, the PID of the n-type rear-emitter configurations has not been investigated in detail so far.

Herein, using a PID acceleration test, we study in detail the PID behavior of modules with a rear-side emitter. To this end, we fabricated rear-emitter configurations by placing n-type single-crystalline Si (sc-Si) bifacial solar cells with the rear side up. This investigated structure is exactly the same as the Al-alloyed rear-side emitter cells except for the formation technique of the p^+ emitters and the rear-side electrode material and shape. Pingel *et al.* [29] already reported on the PID of the n-type c-Si bifacial PV modules; however, they focused mainly on the recovery phenomena of the modules degraded by negative bias. In this contribution, we deal with in detail changes in the current density–voltage (J–V) and the spectral response characteristics of PID-affected modules. Moreover, we focus on the degradation of the modules under positive bias. The dark J–V data are analyzed in detail by fitting to an equation based on the two-diode model [30]. We also briefly discuss possible measures to prevent the PID of the n-type rear-emitter cell modules and investigate the degradation of the modules under positive bias.

2. Experimental

Commercial n-type bifacial sc-Si solar cells composed of silver (Ag) comb-shaped electrode/SiN_x film/p^+ emitter/n-type base/n^+ back surface field/SiN_x film/Ag comb-shaped electrode were cleaved to 20×20 mm^2-sized pieces. Interconnector ribbons were soldered onto the busbars of the front and rear Ag electrodes. The rear-emitter cell modules were fabricated by the lamination of the cells with the p^+ emitter side down. Prepared were stacks composed of conventional tempered cover glass/ethylene-vinyl acetate copolymer (EVA) encapsulant/n-type bifacial sc-Si cell with the p^+ emitter side down/EVA encapsulant/typical backsheet [poly(vinyl fluoride) (PVF)/poly(ethylene terephthalate) (PET)/PVF]. The cover glass had a size of 45×45 mm^2 and contained alkali metals such as Na. The modules were fabricated from the stacks in a module laminator. The lamination process mainly involves two steps: a degassing step that takes place for 5 min and an adhesion step that takes place for 15 min. The stacks were placed with the cover glass side down on a stage heated at 135 °C during lamination. The front-side configuration of the encapsulated cells is exactly the same as that of n-type Al-alloyed rear-emitter cells. The n-type rear-side emitter cell modules used herein show an energy conversion efficiency of approximately 18%.

The PID tests were performed by applying a voltage of −1000 or +1000 V to connected module interconnector ribbons with respect to an aluminum plate placed on the module cover glass in a heating chamber maintained at 85 °C. Herein, we use the terms "negative bias" and "positive bias" for biases that produce the negative and positive potentials of cells with respect to the aluminum plate, respectively. We performed the PID tests for three identical modules under each test condition. This test method and similar ones were widely used and established by many researchers as ways to easily produce PID-affected modules in a short time [17, 21, 28, 31–40]. We use the term "PID stress" here to refer to such bias voltage and temperature stress. In this experiment, humidity in the heating chamber was not controlled during stressing; however, relative humidity in a similar setup [32] is low (approximately 2% RH). We, therefore, disregarded its influence on the performance degradation of the modules, such as the moisture ingress into the modules and the corrosion of the metal parts. Moreover, at the present state, it is unknown for how long the PID test stress corresponds to the duration that generates PID in outdoor large-scale PV systems. We used this PID test for intercomparison between the test samples.

To evaluate the degradation, J–V measurements were conducted under dark and one-sun-illuminated conditions for the modules before and after the PID tests.

Saturation current densities of the first and second diodes J_{01} and J_{02}, respectively, ideality factors of the first and second diodes n_1 and n_2, respectively, parallel resistance R_p, and series resistance R_s were determined by fitting the dark J–V data to the following two-diode equation [30]:

$$J(V) = J_{01}\left[\exp\left(\frac{q(V - JR_s)}{n_1 kT}\right) - 1\right] + J_{02}\left[\exp\left(\frac{q(V - JR_s)}{n_2 kT}\right) - 1\right] + \frac{V - JR_s}{R_p}, \quad (1)$$

where q is the elementary charge, k the Boltzmann constant, and T the absolute temperature. J_{01}, J_{02}, R_p, and R_s were positive, n_1 was restricted to one, and n_2 was limited to greater than one. Additionally, R_s was restricted to $\geq R_{s,initial}$, where $R_{s,initial}$ is the R_s of modules before the PID tests. The two-diode fitting was performed using the statistical software Igor Pro 6 (WaveMetrics, Inc.). To estimate the spectral response losses of the degraded modules, external quantum efficiency (EQE) measurements were conducted before and after the PID tests.

3. Results

3.1. Degradation behavior under negative bias

It is so far reported that applying a high negative bias to cells leads to the degradation of many types of PV modules, such as conventional p-type c-Si modules [10–12], n-type front-emitter c-Si modules [28], n-type IBC c-Si modules [26], n-type IBC c-Si modules with front-floating emitter [27], amorphous Si (a-Si) modules [32, 41], Cu(In,Ga)Se_2 cells [42] and modules [32, 41], and CdTe modules [43]. Herein, we first clarify how the J–V characteristics and the EQEs of the n-type rear-emitter PV modules change by applying negative bias.

Fig. 1 presents the representative one-sun-illuminated J–V curves for the n-type rear-emitter modules before and after the PID tests when applying a voltage of −1000 V to the cell with respect to the front surface of the cover glass. The modules exhibit a significant drop in V_{oc} and a relatively small drop in J_{sc}, which is consistent with the result of a previous study [29]. However, a decrease in FF is seen in this experiment, which was not observed in the previous studies [29].

Fig. 2 shows the dependence of $J_{sc}/J_{sc,0}$, $V_{oc}/V_{oc,0}$, FF/FF_0, and $P_{max}/P_{max,0}$ of the n-type rear-emitter modules on PID-stress duration, where the subscript 0 indicates the initial value and P_{max} is the maximum output power. The values plotted in Fig. 2 are calculated from the one-sun-illuminated J–V data of three identical modules, including the module whose J–V curves are shown in Fig. 1. As mentioned above, all the parameters decrease with increasing PID-stress duration. In particular, V_{oc} significantly decreases within the first hour, indicating that

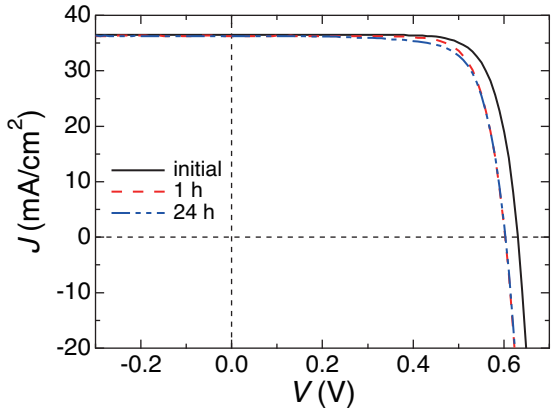

Figure 1: Representative one-sun-illuminated J–V characteristics of the n-type rear-emitter PV modules before and after the PID tests applying −1000 V.

the PID of n-type rear-emitter modules is characterized by a reduction in V_{oc}. V_{oc} is then saturated, even after longer PID tests. Similar saturation behavior is also observed in J_{sc} and FF.

Fig. 3 gives the representative dark J–V curves of the n-type rear-emitter cell modules before and after the PID tests, and Fig. 4 shows the dependence of J_{01}, J_{02}, n_2, and R_p on the PID stress duration. These parameters are obtained by fitting the dark J–V data to the two-diode model [30]; thus, for instance, R_p does not generally correspond to that simply obtained from the slope of the dark J–V curves under the reverse bias. R_s is considerably low and remain almost unchanged during the PID tests (not shown here). As observed in Fig. 3, the current density significantly increases both under reverse and forward bias with PID-stress duration. The increase in the current density corresponds to the increases in J_{01} and J_{02} displayed in Fig. 4, which implies that PID stress shortens the minority carrier lifetime of the cells. J_{01} increases after the PID test for 1 h, indicating enhanced recombination in the emitter and/or the base in the solar cells. n_2 and $1000/R_p$ slightly increase with PID-stress duration. However, unlike p-type c-Si modules, n-type rear-emitter modules do not exhibit significant increases in $1000/R_p$ and n_2. This is probably because the p–n junction in rear-emitter configurations is less influenced by PID stress, as compared with p-type c-Si cells with a front emitter. The increases in $1000/R_p$, and J_{02} and n_2 may be due to the introduction of Na through the unpassivated edge of the cells (Section 4.1).

Fig. 5 shows the EQE spectra of unaffected and degraded rear-side emitter PV

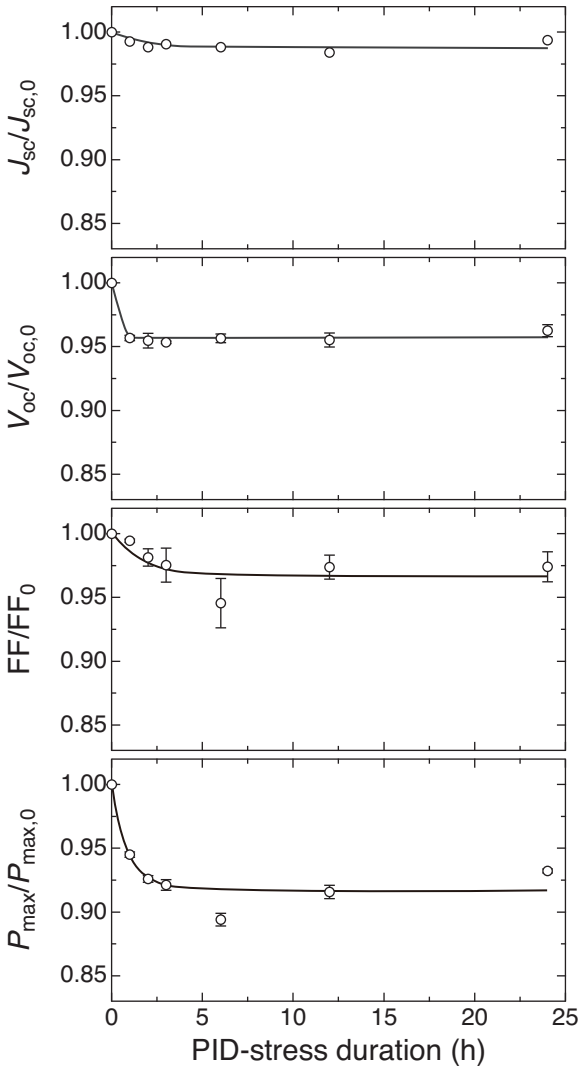

Figure 2: Dependence of $J_{sc}/J_{sc,0}$, $V_{oc}/V_{oc,0}$, FF/FF$_0$, and $P_{max}/P_{max,0}$ of the n-type rear-emitter modules on negative-biasing PID-stress duration. Each data point shows the mean value for three modules, and each error bar corresponds to the standard deviation of the mean. The solid lines are guides to the eye.

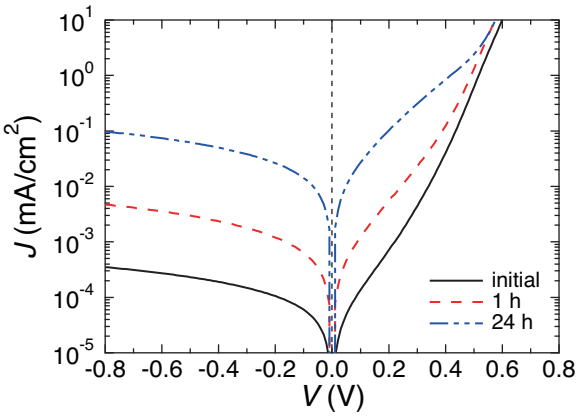

Figure 3: Representative dark J–V characteristics of the rear-side emitter PV modules before and after the PID tests applying −1000 V.

modules as a function of PID-stress duration. A slight decrease in EQE is seen only at a wavelength of 400–600 nm after the PID test for 1 h. The EQE spectrum after the PID test for 24 h in total is considerably similar to that after the PID test for 1 h, corresponding to the saturation behavior observed in J_{sc} given in Fig. 2. The reduction in EQE suggests an enhanced surface recombination of minority carriers due to PID stress. As reported by Hara *et al.* [28], the EQE of the n-type front-emitter PV modules is also reduced at a short-wavelength region after a PID test. The EQE reduction of the rear-emitter cell modules is, however, more slight than that of the n-type front-emitter solar cells.

3.2. Degradation behavior under positive bias

Prior work revealed that n-type IBC PV modules exhibit a significant loss in output power accompanied by reduction of J_{sc} and V_{oc} under positive voltage stress [25]. This phenomenon is generally referred to as the "polarization effect" [25]. For the n-type rear-emitter cell modules, a configuration near the front surface involves Ag electrode/SiN_x passivation layer/n^+ front surface field/n-type base. This structure is very similar to that of the n-type IBC solar cells except for the existence of the front Ag electrode. The n-type rear-emitter cell modules may, therefore, degrade due to positive bias. To confirm this, we conduct the PID tests applying +1000 V to the cell with respect to the front surface of the cover glass.

Fig. 6 shows the representative one-sun-illuminated and dark J–V curves of the n-type rear-emitter cell modules before and after the PID tests by applying

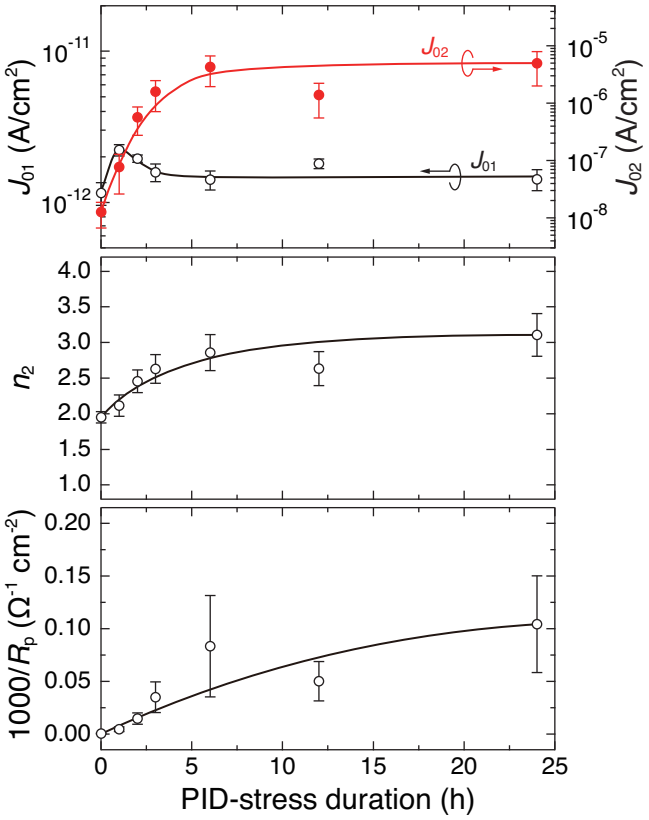

Figure 4: Dependence of J_{01}, J_{02}, n_2, and $1000/R_p$ of the n-type rear-emitter modules on negative-biasing PID-stress duration. Each data point shows the mean value for three modules, and each error bar corresponds to the standard deviation of the mean. The solid lines are guides to the eye.

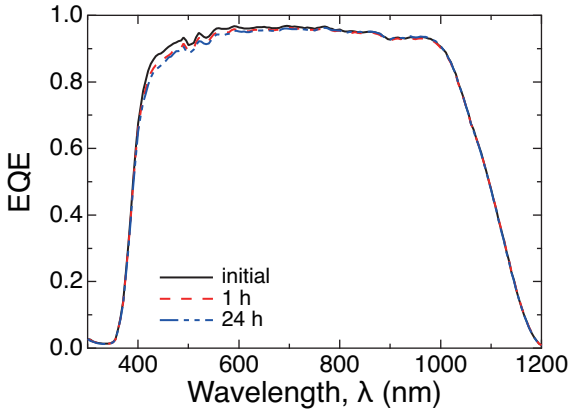

Figure 5: EQE spectra of the rear-emitter PV modules before and after the PID tests applying −1000 V for 1 and 24 h.

+1000 V. The J–V curves exhibit slight decreases in J_{sc}, V_{oc}, and FF after the PID tests. As shown in Fig. 6b, the current density increases both under reverse and forward bias after the PID test for 24 h. The two-diode fitting of the dark J–V curves clarifies that J_{02} increases from 1.9×10^{-8} A/cm^2 to 2.5×10^{-7} A/cm^2, and n_2 increases from 2.0 to 2.5, which may be the reason behind the reduced FF. By contrast, J_{01} is almost unchanged probably since the drop in V_{oc} is considerably small.

Fig. 7 exhibits the EQE spectra of the n-type rear-emitter cell modules before and after the PID test for 24 h. A slight decrease in EQE is seen at wavelengths of 400–500 nm, indicating that the degradation is attributed to the enhanced surface recombination of minority carriers at the front. The above results imply that n-type rear-emitter cell modules may undergo the polarization effect under positive bias.

3.3. Effect of the insertion of an ionomer thin film

To offer sufficient performance stability, it is important to propose possible techniques for the prevention of the PID. So far, reports suggest that in p-type c-Si cell modules, the PID can be prevented by the chemical composition modification of SiN_x surface passivation layer [11, 33, 44], by the use of quartz cover glass [16], alminosilicate-chemically strengthened glass [34], an acrylic front cover film [35], or cover glass with a TiO_2-coated inner surface [36], by using electric resistance encapsulant [16, 37] instead of the conventional EVA encapsulant, by inserting a

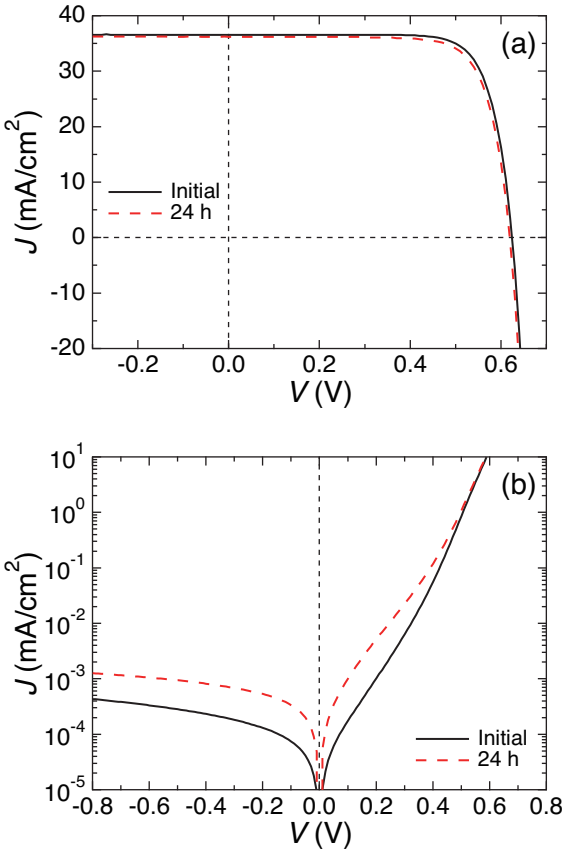

Figure 6: Representative (a) illuminated and (b) dark J–V curves of the n-type rear-emitter PV modules before and after the PID test applying +1000 V for 24 h.

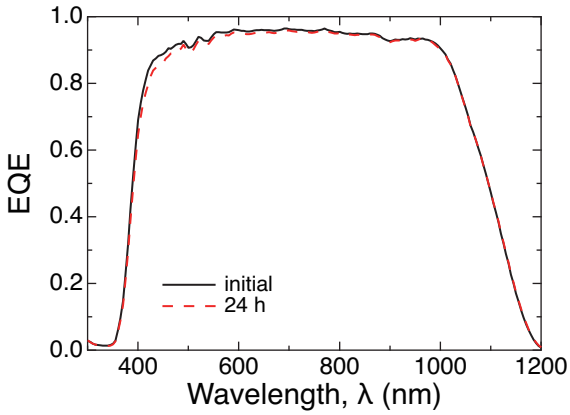

Figure 7: EQE spectra of the rear-emitter PV modules before and after the PID test applying +1000 V for 24 h.

polyethylene [38] or an ionomer [45] thin film between the EVA encapsulant and front cover glass or cells, or by increasing the cross-linkage level or the thickness of the encapsulant [39]. Here, we investigate the effect of the insertion of an ionomer film between the cover glass and EVA encapsulant on the PID under negative bias.

Shown in Fig. 8 are the illuminated J–V curves of the n-type rear-emitter cell module with a 30-μm-thick ionomer film, which is inserted between the cover glass and the EVA encapsulant, before and after the PID test applying -1000 V to the cell with respect to the front surface of the cover glass at 85 °C for 24 h. The module with the ionomer film degrades after the PID test for 24 h. The P_{max} then relatively decreases to 0.94. This implies that the PID of the n-type rear-emitter modules under negative bias cannot be completely prevented by inserting the 30-μm-thick ionomer film.

4. Discussion

4.1. Degradation behavior under negative bias

The degradation of the n-type rear-emitter modules occurs under negative bias and is characterized by a relatively large drop in V_{oc} accompanied by decreases in J_{sc} and FF, as shown in Figs. 1 and 2. The V_{oc} drop is probably attributed to the enhanced surface recombination of minority carriers, since the PID-affected modules exhibit an increase in J_{01} and a decrease in EQE at the short-wavelength

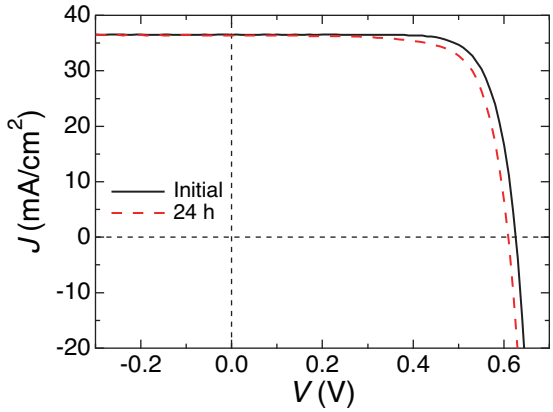

Figure 8: J–V curves of the n-type rear-emitter module with the 30-μm-thick ionomer film before and after the PID test for 24 h.

region, as indicated in Figs. 4 and 5, respectively. The decrease in J_{sc} corresponds to the reduction in EQE at the short-wavelength region. The negative bias might results in the polarization of the surface passivation layer of cells and Na introduction into the cells. In the n-type rear-emitter modules, the former may not be detrimental to the surface passivation, because expected polarization produces a positively charged region at the n-type surface and repels the minority carriers, holes. The enhanced surface recombination of minority carriers may therefore be caused by the introduction of Na into the surface region of the cells. For p-type c-Si modules, stacking faults are decorated by such Na. If such Na-decorated stacking faults penetrate the p–n junctions, they behave as two-dimensional electrical conductive layers [18, 22]. Contrarily, n-type rear-emitter cell modules have the p–n junction at the rear side. Because of this, the short-circuiting of the p–n junctions does not take place. Instead, the Na-decorated stacking faults may behave as recombination centers at the front n-type region, whereby J_{01} is increased. Naumann *et al.* [26] suggested that, in n-type IBC c-Si PV cells, Na-decorated stacking faults increase the surface recombination velocity of minority carriers. The root cause of the PID of n-type rear-emitter c-Si PV modules may be identical to that of the PID of n-type IBC c-Si PV modules.

The degradation behavior is similar to that of the n-type front-emitter c-Si modules [28], whereas V_{oc} and J_{sc} decreases of the n-type rear-emitter modules are smaller than those of the n-type front-emitter PV modules. The degradation of both modules is probably attributed to the surface recombination of the minor-

ity carriers. Furthermore, the degradation of the n-type front-emitter PV modules might originate from the surface polarization of the cells [28]. However, there is a possibility that Na atoms are introduced into the p^+ front emitter and activate recombination there. We now assume that such Na atoms introduced into Si also contribute to the PID of the n-type front-emitter cell modules. Based on this hypothesis, the difference may be due to the combination of the two effects, the surface polarization and Na introduction. In other words, the n-type rear-emitter modules may be affected only by the Na introduction, whereas the front-emitter modules may degrade both by the effects of the surface polarization and Na introduction. Furthermore, this hypothesis can consistently explain the difference in the n-type front-emitter and n-type rear-emitter modules in terms of a difference in the capture cross-sections between electrons and holes. Na impurities generally produce donor-like defects in Si [46]. Namely, the Na impurities are positively charged in Si; thereby, a relatively large capture cross-section of electrons can be provided. Hence, when Na atoms are introduced in the p^+ emitters of the n-type front-emitter cell modules, they efficiently capture minority carriers, electrons. This leads to the significant shortening of the minority carrier lifetime in a p-type region, and results in significant reduction in V_{oc} and J_{sc} of solar cells. Therefore, n-type front-emitter modules can be significantly degraded by Na introduction. However, Na impurities are less efficient in the front n-type region for n-type rear-emitter modules, because Na atoms less efficiently capture minority carriers of n-type semiconductors, holes. Therefore, the V_{oc} and J_{sc} losses of n-type rear-emitter modules are not significant, compared with the n-type front-emitter cell modules.

In Figs. 1 and 2, we observe the saturation behavior of drops in J_{sc}, V_{oc}, and FF. This kind of saturation behavior is not observed in the conventional p-type c-Si PV modules. This saturation behavior may be an advantage of the n-type rear-emitter configurations, because, at least, the saturated efficiency is ensured as power generation performance in PV systems. At present, it is unclear why the saturation effect occurs.

As shown in Figs. 1 and 2, FF decreases by PID-stress. This was not observed in the previous study [29]. Generally, FF is mainly related to R_s, R_p, and J_{02} and n_2. In our experiment, R_s was considerably low and almost unchanged during PID tests. The decrease in FF can therefore be attributed to the increases in $1000/R_p$ and/or J_{02} and n_2. However, R_p was sufficiently high (approximately 10 $k\Omega \cdot cm^2$ after the PID tests for 24 h in total), and such a high R_p does not influence FF. Hence, the drop in FF is caused by the increases in J_{02} and n_2. J_{02} and n_2 generally indicate the degree of recombination currents, and large J_{02} and n_2 imply

that the recombination currents are more dominant in the total currents in p–n junctions. In this context, the PID stress from the front cover glass side should affect the rear-side p–n junction of the n-type rear-emitter solar cells. In terms of the configuration of the cells, Na introduced through the front surface of cells cannot probably reach the rear-side p–n junction through the thicker n-type base region. A reason for the increased J_{02} and n_2 might be the Na introduction into the rear-side p–n junction through the edge surface. The edge surface is unpassivated, and Na can therefore be easily introduced through the cell edge. Such Na atoms may cause the enhancement of depletion region recombination. Herein, we used 20×20 mm^2-sized small-area cells. This may explain why the drop in FF is seen only in our experiment, since such small-area cells are generally affected by the edge region.

4.2. Degradation behavior under positive bias

As mentioned above, n-type rear-emitter cells have very similar front structure with n-type IBC solar cells. Because of this, the polarization effect reported by Swanson *et al.* [25] may also occur in n-type rear-emitter cell modules. As shown in Fig. 6a, the n-type rear-emitter module is slightly degraded by the applied positive bias, and the degradation is characterized by slight decrease in J_{sc} and V_{oc}. As observed in Fig. 7, the EQE is decreased at the short-wavelength region after the PID test, implying that the decreases in J_{sc} and V_{oc} are caused by the enhancement of the surface recombination of minority carriers. The degradation behavior under positive bias is considerably similar to that of the n-type IBC solar cells [25]. These probably demonstrate that n-type rear-emitter modules are subjected to the polarization effect. However, the modules may tend to be less affected by the polarization effect compared to n-type IBC PV modules. Note that the root cause of the polarization effect has not been clarified so far. Therefore much additional work is required to elucidate the degradation phenomenon occurring under positive bias.

We now briefly consider the high stability of the n-type rear-emitter modules under positive bias. As explained below, the presence of the front electrode might be related to the higher stability under positive bias. Applying a positive voltage stress on the cells with respect to the frame, non-zero leakage currents are observed between the frame and the cells [25]. Such currents can lead to the accumulation of negative charges on the surface passivation layer, and these negative charges polarize the passivation layer [25]. For rear-emitter cell modules, the negative charges can also reach the front surface of the cells. However, in the presence of the front electrode, some of the negative charges are collected by them and may

then neutralized on the positively charged electrode surfaces. Moreover, negative charges reaching the passivation layer might also move to the electrode through the surface of the layer.

4.3. Effect of the insertion of an ionomer thin film

It was reported that the PID of p-type c-Si PV modules can be completely prevented by inserting a polymer film, such as polyethylene [38] or ionomer [45]. As indicated in Fig. 8, however, the insertion of the 30-μm-thick ionomer film does not prevent the PID of the n-type rear-emitter module. Such an inserted ionomer film significantly reduces Na ion migration rate [45]. However, ionomer encapsulants cannot suppress the migration of Na atoms to cells at all [40]. Na atoms may thus reach the cell surface even in the presence of an ionomer film, which might be assisted by a negative bias. The n-type rear-emitter modules might tend to degrade by fewer doses of Na atoms. On the basis of a model proposed by Naumann *et al.* [47], PID suppression effects by high-electric-resistance encapsulant are caused by increased resistance. The above result may suggest that higher resistance is required for preventing the PID. The increased resistance of encapsulation makes voltages across the SiN_x layers low, implying that the PID of n-type rear-emitter c-Si PV modules tends to occur under a relatively small bias voltage. To determine possible measures to prevent the PID, we must further investigate the effect of module components on the PID behavior of the n-type rear-emitter modules.

4.4. Comparing PID resistance with that of other types

In terms of installation in VLS-PV systems, it is important to compare the PID resistance of the n-type rear-emitter modules with that of other types of modules. We reported the test results of multi-crystalline Si (mc-Si), a-Si, and CIGS modules [32]. After the tests within 1 day under the same temperature and voltage conditions, $P_{\mathrm{max}}/P_{\mathrm{max},0}$ of the mc-Si, a-Si, and CIGS decrease to 0.04–0.4, 0.23, and 0.95, respectively. By contrast, $P_{\mathrm{max}}/P_{\mathrm{max},0}$ of the n-type rear-emitter modules drops to 0.93, and the PID-resistance is comparable to that of the CIGS module. These indicate that n-type rear-emitter modules have relatively high PID resistance. This may become an advantage of the n-type rear-emitter modules.

Note that the PID resistance is largely influenced, for instance, by the fabrication conditions and by the test conditions. Our PV modules are placed in a dry environment (typically under a humidity of 2% RH [32]) during our PID test, and the influence of humidity was neglected. However, humidity may strongly affect PID. For instance, CIGS PV modules have higher resistance to our PID tests [32],

whereas they undergo significant degradation under "biased damp heat" conditions, where modules are subjected to intense humidity as well as high temperature and voltage stress [43]. The n-type rear-emitter modules may also show different degradation behavior under different test conditions. We therefore must perform the PID tests of the n-type rear-emitter modules under various conditions.

5. Conclusions

We studied in detail the PID behavior of the n-type rear-emitter modules, using a PID acceleration test. After the PID tests applying −1000 V, the modules show decreases in V_{oc} accompanied by FF and slight J_{sc} reduction. However, the FF reduction may be due to Na introduction through the edge surfaces; in particular, our small-area-cell modules may tend to be more strongly influenced by the properties of the edge region. These indicate that a drop in V_{oc} mainly characterizes the PID of n-type rear-emitter modules. The dark J–V data of the PID-affected modules exhibit increased J_{01}. Furthermore, the EQE spectra of the PID-affected modules are reduced at the short-wavelength region of 400–600 nm. These imply that the decreases in V_{oc} and J_{sc} are due to the enhancement of the surface recombination of minority carriers.

The n-type rear-emitter modules show slight degradation under +1000 V; however, the modules are less influenced by positive bias compared to negative bias. The degradation by positive bias is characterized by decreases in V_{oc} and J_{sc} due to enhanced surface recombination of minority carriers, and is almost identical to the polarization effect observed in n-type IBC PV modules. The high stability under positive bias compared to n-type IBC cell modules might be due to the presence of the front electrode.

Compared to other types of modules such as mc-Si, a-Si, and CIGS PV, the resistance of the n-type rear-emitter modules to our PID test is much higher than those of the mc-Si and a-Si modules, and is comparable to that of the CIGS module. This suggests that n-type rear-emitter modules have higher stability than those of the conventional Si modules and are more suitable for use in VLS-PV systems.

Acknowledgements

This work was supported by the New Energy and Industrial Technology Development Organization (NEDO). The authors would like to thank Yukiko Hara and Sachiko Jonai of AIST for their assistance in module lamination.

References

[1] A. ur Rehman, S. H. Lee, Advancements in n-type base crystalline silicon solar cells and their emergence in the photovoltaic industry, Scientific World J. 2013 (2013) 470347.

[2] J. Zhao, A. Wang, P. P. Altermatt, M. A. Green, J. P. Rakotoniaina, O. Breitenstein, High efficiency PERT cells on n-type silicon substrates, in: Proceedings of the 29th IEEE Photovoltaic Specialists Conference, 19–24 May, New Orleans, LA, USA, 2002, pp. 218–221.

[3] J. Benick, B. Hoex, G. Dingemans, W. M. M. Kessels, A. Richter, M. Hermle, S. W. Glunz, High-efficiency n-type silicon solar cells with front side boron emitter, in: Proceedings of the 24th European Photovoltaic Solar Energy Conference, 21–25 September, Hamburg, Germany, 2009, pp. 863–870.

[4] T. Mishima, M. Taguchi, H. Sakata, E. Maruyama, Development status of high-efficiency HIT solar cells, Sol. Enegry Mater. Sol. Cells 95 (2011) 18–21.

[5] T. Kinoshita, D. Fujishima, A. Yano, A. Ogane, S. Tohoda, K. Matsuyama, Y. Nakamura, N. Tokuoka, H. Kanno, H. Sakata, M. Taguchi, E. Maruyama, The approaches for high efficiency HIT solar cell with very thin (<100 μm) silicon wafer over 23%, in: Proceedings of the 26th European Photovoltaic Solar Energy Conference and Exhibition, 5–9 September, Hamburg, Germany, 2011, pp. 871–874.

[6] M. Taguchi, A. Yano, S. Tohoda, K. Matsuyama, Y. Nakamura, T. Nishiwaki, K. Fujita, E. Maruyama, 24.7% record efficiency HIT solar cell on thin silicon wafer, IEEE J. Photovoltaics 4 (2014) 96–99.

[7] C. Schmiga, H. Nagel, J. Schmidt, 19% efficient n-type Czochralski silicon solar cells with screen-printed aluminium-alloyed rear emitter, Prog. Photovoltaics: Res. Appl. 14 (2006) 533–539.

[8] C. Schmiga, M. Hörteis, M. Rauer, K. Meyer, J. Lossen, H.-J. Krokoszinski, M. Hermle, S. W. Glunz, Large-area n-type silicon solar cells with printed contacts and aluminium-alloyed rear emitter, in: Proceedings of the 24th European Photovoltaic Solar Energy Conference and Exhibition, 21–25 September, Hamburg, Germany, 2009, pp. 1167–1170.

[9] C. Schmiga, M. Rauer, M. Rüdiger, K. Meyer, J. Lossen, H.-J. Krokoszinski, M. Hermle, S. W. Glunz, Aluminium-doped p^+ silicon for rear emitters and back surface fields: results and potentials of industrial n-and p-type solar cells, in: Proceedings of the 25th European Photovoltaic Solar Energy Conference and Exhibition/5th World Conference on Photovoltaic Energy Conversion, 6–10 September, Valencia, Spain, 2010, pp. 1163–1168.

[10] S. Pingel, O. Frank, M. Winkler, S. Daryan, T. Geipel, H, Hoehne, J. Berghold, Potential induced degradation of solar cells and panels, in: Proceedings of 35th IEEE Photovoltaic Specialists Conference, June 20–25, Honolulu, HI, USA, 2010, pp. 2817–2822.

[11] J. Berghold, O. Frank, H. Hoehne, S. Pingel, B. Richardson, M. Winkler, Potential induced degradation of solar cells and panels, in: Proceedings of the 25th European Photovoltaic Solar Energy Conference and Exhibition/5th World Conference on Photovoltaic Energy Conversion, 6–10 September, Valencia, Spain, 2010, pp. 3753–3759.

[12] P. Hacke, M. Kempe, K. Terwilliger, S. Glick, N. Call, S. Johnston, S. Kurtz, I. Bennett, M. Kloos, Characterization of multicrystalline silicon modules with system bias voltage applied in damp heat, in: Proceedings of the 25th European Photovoltaic Solar Energy Conference and Exhibition/5th World Conference on Photovoltaic Energy Conversion, 6–10 September, Valencia, Spain, 2010, pp. 3760–3765.

[13] V. Naumann, D. Lausch, C. Hagendorf, Sodium decoration of PID-s crystal defects after corona induced degradation of bare silicon solar cells, Energy Procedia 77 (2015) 397–401.

[14] J. W. Osenbach, S. S. Voris, Sodium diffusion in plasma-deposited amorphous oxygen-doped silicon nitride (a-SiON:H) films, J. Appl. Phys. 63 (1988) 4494–4500.

[15] M. Wilson, A. Savtchouk, P. Edelman, D. Marinskiy, J. Lagowski, Drift characteristics of mobile ions in SiN_x films and solar cells, Sol. Energy Mater. Sol. Cells 142 (2015) 102–106.

[16] P. Hacke, K. Terwilliger, R. Smith, S. Glick, J. Pankow, M. Kempe, S. Kurtz, I. Bennett, M. Kloos, System voltage potential-induced degradation mechanisms in PV modules and methods for test, in: Proceedings of the 37th IEEE

Photovoltaic Specialists Conference, 19–24 June, Seattle, WA, USA, 2011, pp. 814–820.

[17] C. Taubitz, M. Schütze, M. B. Koentopp, Towards a kinetic model of potential-induced shunting, in: Proceedings of the 27th European Photovoltaic Solar Energy Conference and Exhibition, 24–28 September, Frankfurt, Germany, 2012, pp. 3172–3176.

[18] V. Naumann, D. Lausch, A. Hähnel, J. Bauer, O. Breitenstein, A. Graff, M. Werner, S. Swatek, S. Großer, J. Bagdahn, C. Hagendorf, Explanation of potential-induced degradation of the shunting type by Na decoration of stacking faults in Si solar cells, Sol. Energy Mater. Sol. Cells 120 (2014) 383–389.

[19] V. Naumann, C. Hagendorf, S. Grosser, M. Werner, J. Bagdahn, Micro structural root cause analysis of potential induced degradation in c-Si solar cells, Energy Procedia 27 (2012) 1–6.

[20] J. Bauer, V. Naumann, S. Großer, C. Hagendorf, M. Schütze, O. Breitenstein, On the mechanism of potential-induced degradation in crystalline silicon solar cells, Phys. Status Solidi: Rapid Res. Lett. 6 (2012) 331–333.

[21] V. Naumann, D. Lausch, S. Großer, M. Werner, S. Swatek, C. Hagendorf, J. Bagdahn, Microstructural analysis of crystal defects leading to potential-induced degradation (PID) of Si solar cells, Energy Procedia 33 (2013) 76–83.

[22] V. Naumann, D. Lausch, A. Graff, M. Werner, S. Swatek, J. Bauer, A. Hähnel, O. Breitenstein, S. Großer, J. Bagdahn, C. Hagendorf, The role of stacking faults for the formation of shunts during potential-induced degradation of crystalline Si solar cells, Phys. Status Solidi: Rapid Res. Lett. 7 (2013) 315–318.

[23] D. Lausch, V. Naumann, O. Breitenstein, J. Bauer, A. Graff, J. Bagdahn, C. Hagendorf, Potential-induced degradation (PID): Introduction of a novel test approach and explanation of increased depletion region recombination, IEEE J. Photovoltaics 4 (2014) 834–840.

[24] B. Ziebarth, M. Mrovec, C. Elsässer, P. Gumbsch, Potential-induced degradation in solar cells: Electronic structure and diffusion mechanism of sodium in stacking faults of silicon, J. Appl. Phys. 116 (2014) 093510.

[25] R. Swanson, M. Cudzinovic, D. DeCeuster, V. Desai, J. Jürgens, N. Kaminar, W. Mulligan, L. Rodrigues-Barbosa, D. Rose, D. Smith, A. Terao, K. Wilson, The surface polarization effect in high-efficiency silicon solar cells, in: Technical Digest of the 15th Photovoltaic Science and Engineering Conference, 10–15 October, Shanghai, China, 2005, pp. 410–411.

[26] V. Naumann, T. Geppert, S. Großer, D. Wichmann, H.-J. Krokoszinski, M. Werner, C. Hagendorf, Potential-induced degradation at interdigitated back contact solar cells, Energy Procedia 55 (2014) 498–503.

[27] A. Halm, A. Schneider, V. D. Mihailetchi, L. J. Koduvelikulathu, L. M. Popescu, G. Galbiati, H. Chu, R. Kopecek, Potential-induced degradation for encapsulated n-type IBC solar cells with front floating emitter, Energy Pocedia 77 (2015) 356–363.

[28] K. Hara, S. Jonai, A. Masuda, Potential-induced degradation in photovoltaic modules based on n-type single crystalline Si solar cells, Sol. Energy Mater. Sol. Cells 140 (2015) 361–365.

[29] S. Pingel, S. Janke, O. Frank, Recovery methods for modules affected by potential induced degradation (PID), in: proceedings of the 27th European Photovoltaic Solar Energy Conference and Exhibition, 24–28 September, Frankfurt, Germany, 2012, pp. 3379–3383.

[30] M. Wolf, G. T. Noel, R. J. Stirn, Investigation of the double exponential in the current–voltage characteristics of silicon solar cells, IEEE Trans. Electron Devices 24 (1977) 419–428.

[31] S. Hoffmann, M. Koehl, Effect of humidity and temperature on the potential-induced degradation, Prog. Photovoltaics: Res. Appl. 22 (2014) 173–179.

[32] S. Yamaguchi, S. Jonai, K. Hara, H. Komaki, Y. Shimizu-Kamikawa, H. Shibata, S. Niki, Y. Kawakami, A. Masuda, Potential-induced degradation of Cu(In,Ga)Se_2 photovoltaic modules, Jpn. J. Appl. Phys. 54, (2015) 08KC13.

[33] S. Koch, D. Nieschalk, J. Berghold, S. Wendlandt, S. Krauter, P. Grunow, Potential induced degradation effects on crystalline silicon cells with various antireflective coatings, in: Proceedings of the 27th European Photovoltaic Solar Energy Conference and Exhibition, 24–28 September, Frankfurt, Germany, 2012, pp. 1985–1990.

[34] M. Kambe, K. Hara, K. Mitarai, S. Takeda, M. Fukawa, N. Ishimaru, M. Kondo, PID-free c-Si PV module using alminosilicate chemically strengthened glass, in: Proceedings of the 28th European Photovoltaic Solar Energy Conference and Exhibition, 30 September–4 October, Paris, France, 2013, pp. 2861–2864.

[35] T. Kajisa, H. Miyauchi, K. Mizuhara, K. Hayashi, T. Tokimitsu, M. Inoue, K. Hara, A. Masuda, Novel lighter weight crystalline silicon photovoltaic module using acrylic-film as a cover sheet, Jpn. J. Appl. Phys. 53 (2014) 092302.

[36] K. Hara, H. Ichinose, T. N. Murakami, A. Masuda, Crystalline Si photovoltaic modules based on TiO_2-coated cover glass against potential-induced degradation, RSC Adv. 4 (2014) 44291–44295.

[37] S. Koch, J. Berghold, O. Okoroafor, S. Krauter, P. Grunow, Encapsulation influence on the potential induced degradation of crystalline silicon cells with selective emitter structures, in: Proceedings of the 27th European Photovoltaic Solar Energy Conference and Exhibition, 24–28 September, Frankfurt, Germany, 2012, pp. 1991–1995.

[38] K. Hara, S. Jonai, A. Masuda, Crystalline Si photovoltaic modules functionalized by a thin polyethylene film against potential and damp-heat-induced degradation, RSC Adv. 5 (2015) 15017–15023.

[39] S. Jonai, K. Hara, Y. Tsutsui, H. Nakahama, A. Masuda, Relationship between cross-linking conditions of ethylene vinyl acetate and potential induced degradation for crystalline silicon photovoltaic modules, Jpn. J. Appl. Phys. 54 (2015) 08KG01.

[40] A. Masuda, Y. Hara, S. Jonai, Consideration on Na diffusion and recovery phenomena in potential-induced degradation for crystalline Si photovoltaic modules, Jpn. J. Appl. Phys. 55 (2016) 02BF10.

[41] P. Lechner, S. Hummel, D. Geyer, H.-D. Mohring, PID-behaviour of thin-film and c-Si PV-modules, in: Proceedings of the 28th European Photovoltaic Solar Energy Conference and Exhibition, 30 September–4 October, Paris, France, 2013, pp. 2810–2815.

[42] V. Fjällström, P. M. P. Salomé, A. Hultqvist, M. Edoff, T. Jarmar, B. G. Aitken, K. Zhang, K. Fuller, C. K. Williams, Potential-induced degradation

of $CuIn_{1-x}Ga_xSe_2$ thin film solar cells, IEEE J. Photovoltaics 3 (2013) 1090–1094.

[43] Z. Xiong, T. M. Walsh, A. G. Aberle, PV module durability testing under high voltage biased damp heat conditions, Energy Pocedia 8 (2011) 384–389.

[44] H. Nagel, A. Metz, K. Wangemann, Crystalline Si solar cells and modules featuring excellent stability against potential-induced degradation, in: Proceedings of the 26th European Photovoltaic Solar Energy Conference and Exhibition, 5–9 September, Hamburg, Germany, 2011, pp. 3107–3112.

[45] J. Kapur, K. M. Stika, C. S. Westphal, J. L. Norwood, B. Hamzavytehrany, Prevention of potential-induced degradation with thin ionomer film, IEEE J. Photovoltaics 5 (2015) 219–223.

[46] S. M. Sze, K. K. Ng, Physics of semiconductor devices, third ed., Wiley, New York, 2006, p. 23.

[47] V. Naumann, K. Ilse, C. Hagendorf, On the discrepancy between leakage currents and potential-induced degradation of crystalline silicon modules, in: Proceedings of the 28th European Photovoltaic Solar Energy Conference and Exhibition, 30 September–4 October, Paris, France, 2013, pp. 2994–2997.